

# Activity-dependent liberation of synaptic neuropeptide vesicles

Dinara Shakiryanova<sup>1,4</sup>, Arvonn Tully<sup>1,4</sup>, Randall S Hewes<sup>2</sup>, David L Deitcher<sup>3</sup> & Edwin S Levitan<sup>1</sup>

Despite the importance of neuropeptide release, which is evoked by long bouts of action potential activity and which regulates behavior, peptidergic vesicle movement has not been examined in living nerve terminals. Previous *in vitro* studies have found that secretory vesicle motion at many sites of release is constitutive: Ca<sup>2+</sup> does not affect the movement of small synaptic vesicles in nerve terminals or the movement of large dense core vesicles in growth cones and endocrine cells. However, *in vivo* imaging of a neuropeptide, atrial natriuretic factor, tagged with green fluorescent protein in larval *Drosophila melanogaster* neuromuscular junctions shows that peptidergic vesicle behavior in nerve terminals is sensitive to activity-induced Ca<sup>2+</sup> influx. Specifically, peptidergic vesicles are immobile in resting synaptic boutons but become mobile after seconds of stimulation. Vesicle movement is undirected, occurs without the use of axonal transport motors or F-actin, and aids in the depletion of undocked neuropeptide vesicles. Peptidergic vesicle mobilization and post-tetanic potentiation of neuropeptide release are sustained for minutes.

Neuropeptides are synthesized in the neuronal cell body, packaged in large dense core vesicles (LDCVs) and transported to nerve terminals. There they accumulate with little docking until they are released away from active zones, affecting mood, behavior, development and peripheral tissues. This release typically occurs slowly over long periods in response to repetitive firing. In contrast, classical transmitters are packaged in small synaptic vesicles (SSVs) at the nerve terminal and undergo fast phasic release at active zones in response to single action potentials. Furthermore, the supply of SSVs is unlimited because they are locally produced by endocytosis and refilled by transporters. Thus, peptidergic and classical neurotransmission are distinct types of neurosecretion that occur within single nerve terminals<sup>1–4</sup>.

Despite these differences, the release of small-molecule transmitters and the release of peptide transmitters are based on conserved features. For example, the release of both neuropeptides and classical transmitters are triggered by Ca<sup>2+</sup> influx through voltage-gated Ca<sup>2+</sup> channels. Likewise, both fast and peptidergic transmissions rely on the same SNARE proteins<sup>5</sup>. Furthermore, secretory vesicle motion is constitutive at many sites of release: Ca<sup>2+</sup> affects neither the motion of SSVs in retinal, hippocampal and neuromuscular junction nerve terminals, nor the motion of LDCVs in growth cones and endocrine cells<sup>6–11</sup>. Finally, both fast and peptidergic neurotransmission are sensitive to patterned electrical activity. For release of classical transmitters, multiple types of synaptic plasticity have been described<sup>12</sup>. Likewise, the activity dependence of neuropeptide release has been attributed to preparatory, priming and mobilization processes<sup>13–15</sup>. However, the cell biological mechanisms underlying these regulatory effects have not been defined.

Recently, neuropeptide release has been studied by imaging LDCVs directly in living cells. *In vitro* experiments have revealed diverse strategies for recruiting secretory vesicles. For example, predocked LDCVs on the surface of endocrine cells dominate the first few minutes of hormone release, whereas cytoplasmic vesicles tend to be depleted much later<sup>16–18</sup>. In contrast, during peptide release by growth cones, mobile undocked LDCVs are more rapidly depleted<sup>19–21</sup>. Thus far, the behavior of LDCVs in living synapses has not been examined.

*In vivo* imaging of neuropeptide vesicles is now possible with transgenic animals that express green fluorescent protein (GFP)-tagged peptides<sup>22</sup>. In *D. melanogaster*, fluorescence microscopy has been used to detect peptidergic vesicles containing GFP-tagged atrial natriuretic factor (ANF-GFP) in axons and neuromuscular junctions, and Ba<sup>2+</sup>-evoked release of the fluorescent peptide from identified type Ib and III synaptic boutons<sup>23</sup> that differ markedly in their accumulation of LDCVs and SSVs<sup>24,25</sup>. ANF-GFP fluorescence has also been used to assay neuropeptide release evoked by native behaviors<sup>26,27</sup>.

Here we further examine synaptic LDCV behavior and peptide release in *D. melanogaster* nerve terminals. We report robust depletion of synaptic neuropeptide stores based on Ca<sup>2+</sup> influx-triggered liberation of restrained undocked LDCVs. Peptidergic vesicle motion in nerve terminals is undirected and persists for minutes after seconds of activity.

## RESULTS

### Activity-induced synaptic neuropeptide vesicle motion

Synaptic LDCV motion, measured by fluorescence recovery after photobleaching (FRAP) of the fluorescent neuropeptide ANF-GFP, is not constitutive in predominantly peptidergic *D. melanogaster* type

<sup>1</sup>Department of Pharmacology, University of Pittsburgh, Pittsburgh, Pennsylvania 15261, USA. <sup>2</sup>Departments of Zoology and Cell Biology, University of Oklahoma, Norman, Oklahoma 73019, USA. <sup>3</sup>Department of Neurobiology and Behavior, Cornell University, Ithaca, New York 14853, USA. <sup>4</sup>These authors contributed equally to this work. Correspondence should be addressed to E.S.L. (Levitan@server.pharm.pitt.edu).

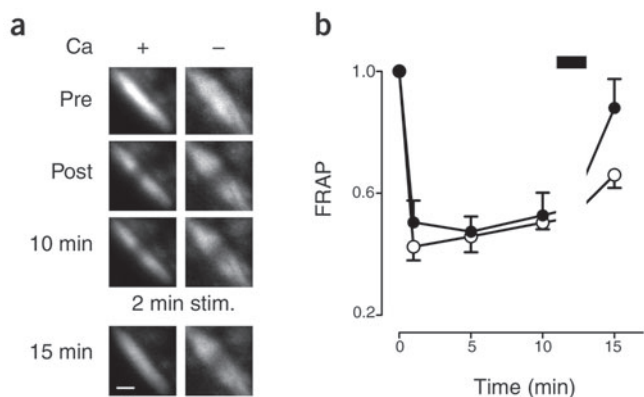


**Figure 1** FRAP reveals  $\text{Ca}^{2+}$ -dependent synaptic neuropeptide vesicle motion in peptidergic type III synapses. **(a)** FRAP in type III boutons depolarized for 2 min in the presence (left) or absence (right) of  $\text{Ca}^{2+}$ . Pre, before photobleaching; Post, after photobleaching; 2 min stim., depolarization for 2 min starting 12 min after the photobleach. Other times reflect time elapsed after photobleaching. Size bar, 2  $\mu\text{m}$ . **(b)** Time course of FRAP obtained with depolarization (indicated by bar) in the presence (●) or absence (○) of  $\text{Ca}^{2+}$  in type III boutons ( $n = 4$ ). The ratio of fluorescence in the photobleached region to a distal unbleached region of the bouton was calculated and then normalized to the ratio before photobleaching to quantify FRAP. Error bars show s.e.m. in this and all following figures.

III boutons. In resting type III boutons, little FRAP occurred within 10 min (**Fig. 1a**), indicating that the mobility of synaptic LDCVs is limited. However, stimulation with a depolarizing version of standard saline<sup>28</sup> (see Methods) induced an increase in neuropeptide in the photobleached region even though total peptide dropped owing to release (**Fig. 1a**). The near completeness of FRAP implies that almost all synaptic peptidergic vesicles were mobilized (**Fig. 1b**). Furthermore, this effect was blocked by removing extracellular  $\text{Ca}^{2+}$  (**Fig. 1a,b**). Thus, LDCV motion in peptidergic synaptic boutons is  $\text{Ca}^{2+}$ -dependent.

This mobilization can be detected without the use of photobleaching in predominantly glutamatergic type Ib boutons that possess some peptidergic vesicles<sup>23–25</sup>. **Figure 2a** shows a wide-field image of a resting type Ib bouton along with a pseudocolor image of the change in fluorescence in 3 s (labeled  $\Delta F$ ). Because measured total neuropeptide fluorescence did not change in this short interval, the  $\Delta F$  panel indicates intrabouton peptidergic vesicle motion. A comparison of the control F and  $\Delta F$  images indicates that few puncta are mobile. However, after electrical stimulation (70 Hz for 15 s) in the high- $\text{Mg}^{2+}/\text{Ca}^{2+}$  saline HL3 (ref. 29), synaptic neuropeptide vesicle motion was enhanced (**Fig. 2a**,  $\Delta F$ , Stim.). Again, these data were obtained during a 3-s interval when there was no substantial change in total GFP-tagged neuropeptide fluorescence, indicating that the alteration in  $\Delta F$  could not be attributed to release. The mobility illustrated in the  $\Delta F$  images was quantified as a mobility index based on the pixel-by-pixel correlation coefficient between sequential images (see Methods). The mobility index was increased by depolarization for 2 min (**Fig. 2b**). A similar effect was elicited by stimulating motor nerves to produce repetitive bursts (intra-burst frequency 70 Hz, burst duration 2 s, mean frequency 35 Hz). However, this

mobilization was abolished by removing extracellular  $\text{Ca}^{2+}$  or by adding the  $\text{Ca}^{2+}$  channel blocker  $\text{Cd}^{2+}$  to the bathing medium (**Fig. 2b**). Thus,  $\text{Ca}^{2+}$  influx evoked by stimulated activity increases synaptic peptidergic vesicle mobility.

Physiological motor neuron activity also stimulates synaptic LDCV motion. Glutamatergic larval neuromuscular junctions *in vivo* are driven by repetitive bursts of motor neuron activity with intraburst frequencies reaching 100 Hz<sup>30,31</sup>. To preserve this central pattern generator (cpg)-driven motor neuron activity, the nervous system was left intact during the dissection in  $\text{Ca}^{2+}$ -free medium. Under these conditions, application of  $\text{Ca}^{2+}$ -containing standard saline re-established cpg-elicited rhythmic muscle contractions. Imaging type Ib boutons between contractions showed that synaptic neuropeptide vesicle mobility increased markedly (**Fig. 2c**). Thus, bursting activity endogenously generated by the central nervous system induced mobilization of synaptic peptidergic vesicles.

### Mobilization by liberation of peptidergic vesicles

Stimulated neuropeptide vesicle motion seems to be the result of liberation of restrained vesicles. First, the extremely limited extent and slow time course of FRAP suggest that LDCVs are immobilized in resting synaptic boutons. Second,  $\text{Ca}^{2+}$ -activated peptidergic vesicle movement in boutons is not polarized. The FRAP results mentioned earlier (**Fig. 1**) show that after stimulation, neuropeptide vesicles move along the lengthwise axonal axis of type III boutons. To test whether these vesicles also move across type III boutons, we used lengthwise edge photobleach profiles (**Fig. 3a**, left). Complete FRAP occurred upon  $\text{Ca}^{2+}$  influx, to again show that essentially all neuropeptide vesicles became mobile (**Fig. 3a**). More importantly, upon stimulation LDCVs moved radially toward the bouton surface. We also detected with wide-field microscopy vesicle redistribution in type Ib boutons that have central regions nearly devoid of neuropeptide (**Fig. 3b**). Confocal microscopy of large type Ib boutons verified that neuropeptide vesicles could move into the 'dark' central regions upon stimulation. For example, neuropeptide fluorescence in the highlighted central region in the bouton in **Figure 3c** increased by 216% even though total neuropeptide fluorescence was reduced by 33%. This implies that mobilized peptidergic vesicles moved away from the bouton surface where exocytosis occurred. As previously mobilized neuropeptide vesicles move toward the center and the periphery and along the length of boutons, their motion

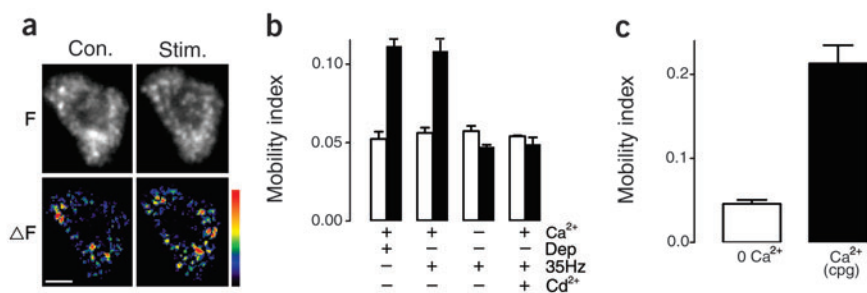


**Figure 2** Activity-dependent neuropeptide vesicle motion in type Ib boutons. **(a)** Top (F), wide-field neuropeptide vesicle fluorescence images of a type Ib bouton before (Con.) and after a 15-s 70-Hz stimulus (Stim.). Lower ( $\Delta F$ ), the change in the top images that occurred in 3 s. Note that release, measured as the change in total neuropeptide fluorescence, in the 3-s interval is negligible and so the  $\Delta F$  images reflect vesicle motion. Size bar, 2  $\mu\text{m}$ . **(b)** Either depolarization or bursting stimulation (35 Hz mean frequency, 70 Hz peak frequency) for 2 min increases neuropeptide vesicle mobility in the presence of  $\text{Ca}^{2+}$ , but this effect is blocked by removal of  $\text{Ca}^{2+}$  or addition of 0.5 mM  $\text{Cd}^{2+}$  ( $n = 6$ ). Open bars, before stimulation; filled bars, after stimulation. **(c)** Mobilization is induced by intrinsic activity. Mobilization is compared before (0  $\text{Ca}^{2+}$ ) and within 2 min after addition of  $\text{Ca}^{2+}$ -containing standard saline to the intact nervous system to enable central pattern generator-induced rhythmic activity ( $\text{Ca}^{2+}$  (cpg)) ( $n = 4$ ).

**Figure 3** Neuropeptide vesicle movement is undirected after liberation.

(a) Depolarization (Stim., indicated by bar in right graph) increases FRAP after tangential lengthwise photobleaching ( $n = 5$ ) of type III boutons. (b,c) Redistribution of neuropeptide vesicles in type Ib synaptic boutons evoked by 2 min of stimulation (Stim.). (b) Wide-field images before and after bursting electrical stimulation. (c) Confocal images before and after depolarization of a large posterior segment type Ib bouton. Equatorial optical sections of confocal stacks are shown. Note that peptidergic vesicles moved into the central region of the bouton indicated by the white outline. Size bars, 2  $\mu\text{m}$ .

appears to be undirected as if LDCVs were freed to diffuse within synaptic boutons.

This conclusion is supported by pharmacological experiments. First, we examined the effects of *N*-ethylmaleimide (NEM), a sulfhydryl reagent that inhibits many myosins and the axonal transport motors kinesin and dynein<sup>32–34</sup>. Earlier work has shown that peptidergic vesicles undergo both anterograde and retrograde transport in larval motor nerves<sup>23</sup>. We found that NEM irreversibly abolished all axonal transport of peptidergic vesicles (Fig. 4a). However,  $\text{Ca}^{2+}$  influx-induced neuropeptide vesicle mobilization and redistribution in type Ib boutons occurred after NEM treatment (Fig. 4b,c). The undirected synaptic neuropeptide vesicle movement that can be induced even after inhibition of many motors is consistent with liberation of restrained LDCVs.

Second, we examined the effect of F-actin-depolymerizing drugs. Cytochalasin D treatment, which is known to be effective in type Ib boutons<sup>35</sup>, did not affect basal or electrically stimulated LDCV motion (Fig. 4d). Basal mobility was also unaffected by mycalolide B, a structurally and mechanistically distinct F-actin-depolymerizing drug that we found effectively blocks muscle contraction (data not shown). In addition, F-actin was difficult to detect in type Ib and III boutons with TRITC-phalloidin labeling (data not shown); its scarcity further suggests the lack of a role for polymerized actin. Because myosins require F-actin for translocation, these results further suggest that mobilization is based on untethering and diffusion rather than motor activation.

**Activity dependence and persistence of vesicle liberation**

Synaptic LDCV mobilization is activity dependent, sustained and reversible. Experiments with type Ib boutons showed that substantial activity is required to initiate peptidergic vesicle movement: 1 s of 70-Hz

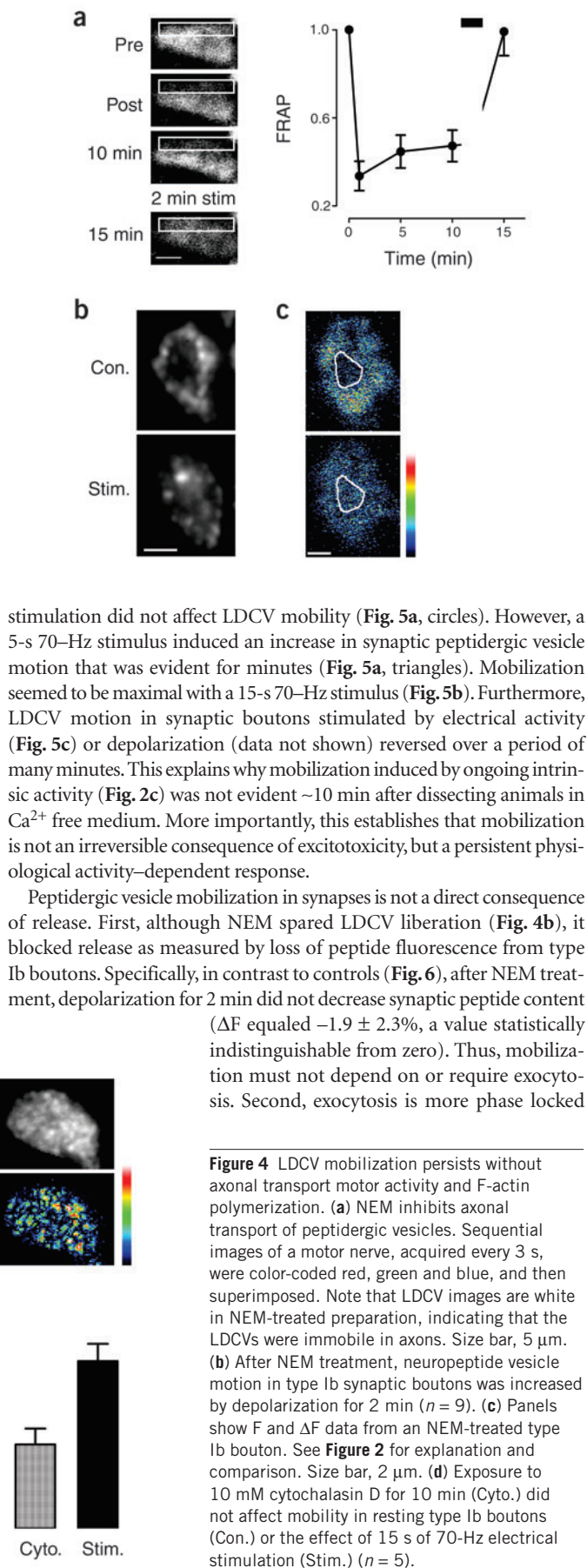


**Figure 4** LDCV mobilization persists without axonal transport motor activity and F-actin polymerization. (a) NEM inhibits axonal transport of peptidergic vesicles. Sequential images of a motor nerve, acquired every 3 s, were color-coded red, green and blue, and then superimposed. Note that LDCV images are white in NEM-treated preparation, indicating that the LDCVs were immobile in axons. Size bar, 5  $\mu\text{m}$ . (b) After NEM treatment, neuropeptide vesicle motion in type Ib synaptic boutons was increased by depolarization for 2 min ( $n = 9$ ). (c) Panels show F and  $\Delta F$  data from an NEM-treated type Ib bouton. See Figure 2 for explanation and comparison. Size bar, 2  $\mu\text{m}$ . (d) Exposure to 10 mM cytochalasin D for 10 min (Cyto.) did not affect mobility in resting type Ib boutons (Con.) or the effect of 15 s of 70-Hz electrical stimulation (Stim.) ( $n = 5$ ).

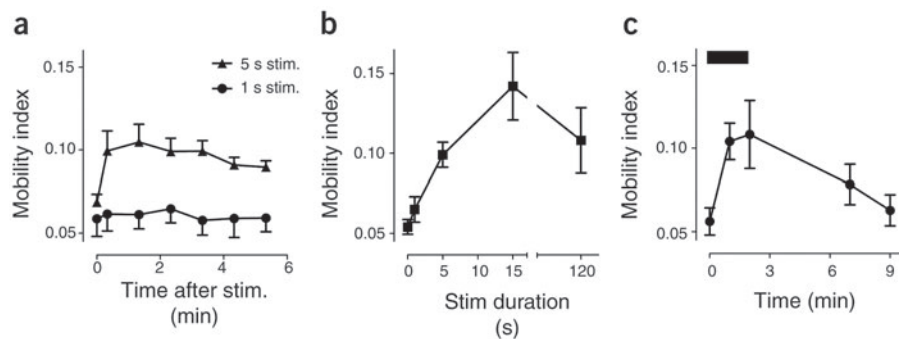


**Figure 5** Persistence and activity dependence of neuropeptide vesicle liberation in type Ib boutons. **(a)** Time course of neuropeptide vesicle motion after 1-s (circles) or 5-s (triangles) 70-Hz stimulations ( $n = 6$ ). **(b)** Dependence of neuropeptide vesicle motion on duration of 70-Hz stimulation ( $n = 6$ ). **(c)** Induction and reversal of mobilization with 2 min of bursting activity (indicated by bar; bursts: 2 s of 70-Hz stimulation, interbursts: 2 s) ( $n = 6$ ).

to electrical activity than LDCV mobility, because mobilization lasted for minutes (**Fig. 5a,c**) whereas release ceased within seconds (**Fig. 6a**). Therefore, mobilization is mechanistically distinct from exocytosis.

### Depletion of liberated synaptic neuropeptide vesicles

Two independent types of experiments suggest that mobilized undocked synaptic LDCVs are depleted within minutes. First, measurement of  $\text{Ca}^{2+}$ -dependent neuropeptide release indicates participation of freed peptidergic vesicles. If mobilized cytoplasmic LDCVs do not participate in release, then the paucity of docked vesicles in *D. melanogaster* type Ib and III synaptic boutons<sup>24,25</sup> should be reflected in meager  $\text{Ca}^{2+}$ -dependent neuropeptide secretion. However, substantial neuropeptide release was triggered within minutes by electrical stimulation of type Ib boutons in HL3 (**Fig. 6b,c**), and even faster release was induced with the stronger stimulus of depolarizing standard saline (**Fig. 6d**). The large extent of neuropeptide release evoked within minutes could not have been produced by a small population of predocked LDCVs, indicating avid participation by liberated synaptic neuropeptide vesicles.

Second, optical sectioning by confocal microscopy revealed neuropeptide depletion away from the nerve terminal surface. For example, neuropeptide levels in the centers of large type III boutons drop markedly with a 3-min depolarization (**Fig. 7a**,  $n = 4$ ). Although light microscopy cannot distinguish between a docked vesicle and a vesicle that is close to but not touching the membrane, the resolution of our optics is sufficient to conclude that any fluorescence more than 290 nm from the bouton surface comes from undocked LDCVs. Thus, the loss of peptide fluorescence in the center of large type III boutons must reflect depletion of undocked peptidergic vesicles. Similar results were obtained in another larger peripheral peptidergic bouton (data not shown,  $n = 5$ ). Likewise, confocal microscopy showed that robust release is accompanied by loss of neuropeptide from throughout large posterior segment

type Ib boutons (**Figs. 7b** and **3c**) that cannot be accounted for by the modest movement of peptidergic vesicles into the centers of these boutons. Thus, confocal microscopy reveals robust depletion away from the bouton surface that could only occur if LDCVs were mobile. As very few peptidergic vesicles are mobile before stimulation and nearly all LDCVs are very mobile after depolarization (**Figs. 1** and **3a**), liberated cytoplasmic neuropeptide vesicles must be depleted in synaptic boutons.

### Post-tetanic potentiation of neuropeptide release

Our demonstration that mobilization persists for minutes led us to test for synaptic plasticity on this time scale. First, we identified type Ib boutons that showed little release in response to a 30-s bout of 3 Hz stimulation. Repeating this weak stimulation evoked reproducible release (**Fig. 8a**). We then examined the effect of a strong stimulation (70 Hz for 15 s) that induces mobilization (**Fig. 5b**). Release in response to the second bout of 3 Hz stimulation was markedly enhanced 2.5 min after the intense bout of activity (**Fig. 8b**). This is significant because it demonstrates a change in release associated with long-term mobilization. Typically, measurements of release have guided the study of regulatory mechanisms. However, in this case, monitoring the inner workings of nerve terminals *in vivo* led to the discovery that peptidergic neurotransmission is subject to minutes-long post-tetanic potentiation.

### DISCUSSION

Neurotransmitter release varies among identified neurons, between classical and peptide cotransmitters, and with patterned activity. Yet the mechanisms that determine the time course and activity dependence of synaptic transmission are not understood. Our experiments with multiple methods and distinct synapse types show that the LDCV motion that aids in robust depletion of synaptic neuropeptide stores is unpolarized and independent of conventional motors. This is reminiscent of SSV behavior in ribbon synapse-containing nerve

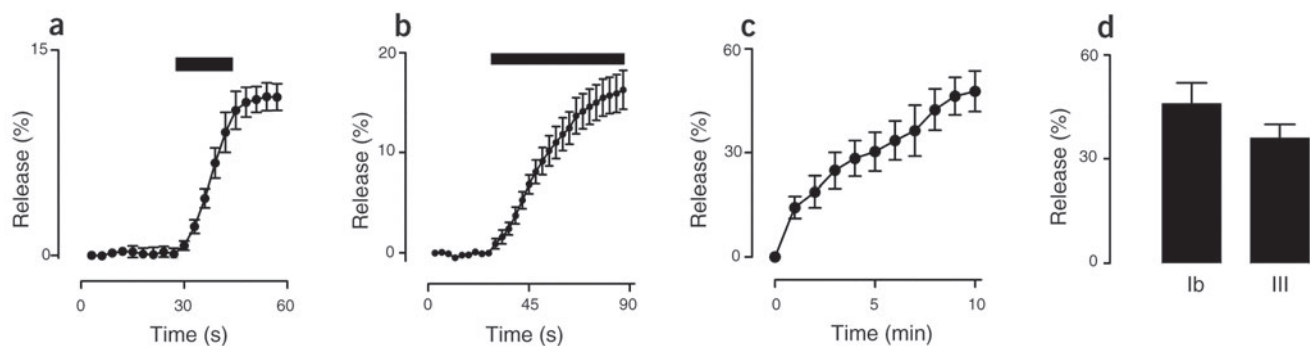


**Figure 6** Robust neuropeptide release by electrical activity or depolarization. Release was measured as the loss of peptide fluorescence (see Methods). **(a)** Release by type Ib boutons in response to a 15-s 70-Hz stimulus ( $n = 5$ ). **(b)** First minute of release by type Ib boutons induced by 70 Hz stimulation in HL3 ( $n = 5$ ). **(c)** Time course of release by type Ib boutons evoked by bursting stimulation (mean frequency 35 Hz) in HL3 ( $n = 6$ ). **(d)** Release evoked by type Ib ( $n = 6$ ) and III ( $n = 5$ ) boutons in 3 min of depolarizing standard saline. Period of stimulation indicated by bar.

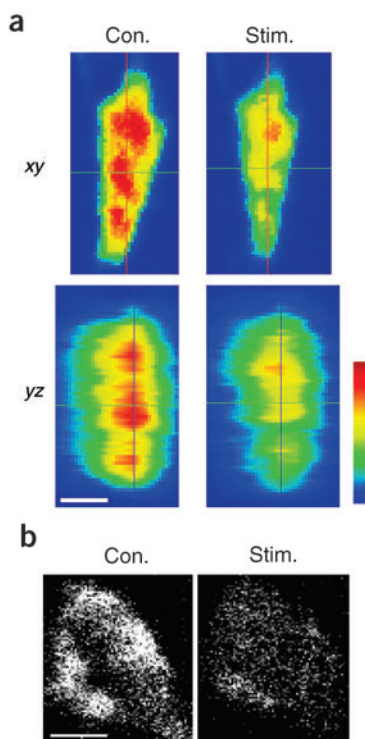


**Figure 7** Depletion of synaptic neuropeptide content detected with confocal microscopy. **(a)** Horizontal (*xy*) and axial (*yz*) confocal sections of a large type III bouton showing neuropeptide fluorescence before and after a 3-min treatment with depolarizing standard saline. **(b)** Horizontal confocal sections of a large type Ib bouton before and after a 3-min treatment with depolarizing standard saline. Size bars, 2  $\mu$ m.

terminals and LDCVs in growth cones<sup>6,7,19,21</sup>. However, peptidergic vesicle motion in synaptic boutons is not constitutive. Rather,  $\text{Ca}^{2+}$  influx induced by depolarization, electrical stimulation or endogenous central pattern generator-induced rhythmic activity increases LDCV movement in nerve terminals. We found this effect dramatic, because FRAP experiments show that nearly all synaptic LDCVs can be mobilized. Furthermore, confocal microscopy and secretion measurements establish that undocked neuropeptide vesicles are efficiently depleted in the first minutes of release. This could not have occurred if synaptic LDCVs remained immobilized and hence unavailable. Therefore, the simplest explanation for our results is that activity-dependent  $\text{Ca}^{2+}$  influx liberates neuropeptide vesicles to diffuse in synaptic terminals to be recruited for exocytosis.

The substantial activity requirement for inducing peptidergic vesicle mobilization, the depletion of mobile LDCVs, and the post-tetanic potentiation that accompanies sustained LDCV mobility all indicate that liberation of restrained synaptic neuropeptide vesicles influences the time course of peptidergic transmission. Indeed, mobilization seems to be a type of activity-dependent priming for the undocked reserve neuropeptide vesicles abundant in nerve terminals. Mobilization may also be relevant for other aspects of the cell biology of peptidergic synapses. For example, liberation may facilitate replacement of old synaptic LDCVs destined for retrograde transport with newly synthesized LDCVs undergoing anterograde transport. It is also conceivable that a similar regulation occurs with SSVs. Although activity-dependent SSV motion has not been detected, it has never been measured within the small clusters of undocked SSVs that surround active zones in canonical fast synapses. Rather, previous FRAP studies with hippocampal

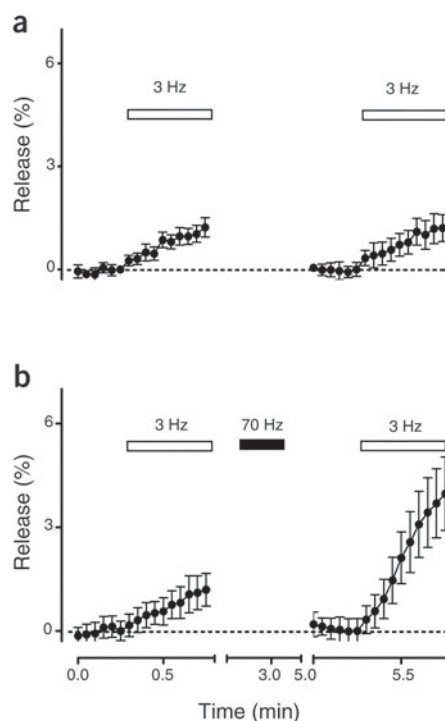


**Figure 8** Post-tetanic potentiation of neuropeptide release by type Ib boutons. **(a)** Release responses to two trials of 30 s of 3-Hz stimulation ( $n = 7$ ). The interval between trials was 5 min. **(b)** Identical stimulation as **a** except that a 15-s 70-Hz stimulus was delivered 2.5 min before the second trial ( $n = 8$ ). Note that the tetanus potentiated the response to 3-Hz stimulation. Release was measured as loss of peptide fluorescence.

neurons and neuromuscular junctions<sup>8,9</sup> had only enough resolution to detect lateral motion between these clusters. Recently, it was proposed that SSVs in the readily releasable pool that supports physiological fast transmission are undocked and mobile within the active zone-associated cloud of SSVs<sup>36</sup>. Thus, it will be important to determine whether the mobilization demonstrated here is unique to synaptic neuropeptide vesicles or operates within the clusters of SSVs adjacent to active zones to potentiate fast transmission.

## METHODS

**Transgenic animals.** All experiments used transgenic *D. melanogaster* (UAS-AnfGFP, FlyBase ID FBti0026990)<sup>23</sup> in which Emerald GFP-tagged atrial natriuretic factor expression was driven by the yeast transcription factor Gal4. To induce expression of the GFP-tagged peptide, these flies were crossed with other transgenic lines that express Gal4 driven by endogenous sequences. For this study, we used the pan-neuronal promoter *elav* (*elav-gal4*, FBti0002575) as was done previously<sup>23</sup> or a sequence upstream of a prohormone convertase gene (*386-gal4*, FBti0020938)<sup>37</sup>. Homozygous female wandering third instar larvae were filleted, and muscle 6, 7 and 12 neuromuscular junction boutons were studied. When necessary for confocal sectioning, the largest type Ib and III boutons were identified based on their GFP fluorescence. Initial experiments were performed in anterior segments A2–A5, but optical sectioning of type Ib boutons was only possible in the more posterior A5 segment where we discovered that these boutons are larger.

**Solutions and stimulation.** Standard saline<sup>28</sup> included 128 mM NaCl, 2 mM KCl, 1.8 mM  $\text{CaCl}_2$ , 4 mM  $\text{MgCl}_2$ , 35.5 mM sucrose, 5 mM sodium HEPES, pH 7.2. The high  $\text{Mg}^{2+}/\text{Ca}^{2+}$  saline HL<sup>39</sup> contained 70 mM NaCl, 5 mM KCl, 1.5 mM  $\text{CaCl}_2$ , 20 mM  $\text{MgCl}_2$ , 10 mM  $\text{NaHCO}_3$ , 5 mM trehalose, 115 mM sucrose, 5 mM sodium HEPES, pH 7.2. Dissections were performed in the presence of 0-Ca saline in which  $\text{Ca}^{2+}$  was excluded or substituted with

0.5 mM EGTA. Boutons were electrically stimulated via a suction electrode on the motor nerve after reintroduction of  $\text{Ca}^{2+}$ . To minimize spontaneous muscle contractions that disrupt imaging during electrical stimulation experiments, the ventral ganglion was cut to prevent input from a central pattern generator<sup>31</sup>, HL3 was used, and 10 mM glutamate was included in the saline to desensitize postsynaptic receptors. Control experiments showed that glutamate did not affect synaptic LDCV movement and was not required for induction of motion. Indeed, data in **Figures 1, 3a** and **4c** were obtained without glutamate. These measures were necessary because electrically evoked neuropeptide release was compromised by cutting nerves. Bursting stimulation was generated by alternating between 2-s trains (for example, 5 V for 0.5 ms at 70 Hz) and 2-s silent periods. In most depolarization experiments, the preparation was switched directly from a 0 Ca saline into 'depolarizing standard saline' in which 85 mM NaCl was replaced with KCl. However, the  $\text{K}^+/\text{Na}^+$  substitution was performed with HL3 (to generate 'depolarizing HL3') for the direct comparison of depolarization to electrical stimulation (**Fig. 2b**). Because depolarization normally elicits muscle contraction, images were acquired after removing the excess bath KCl except after treatment with 1 mM NEM for 15 min, which irreversibly inhibits muscle contraction.

**Imaging.** Neuromuscular junctions were imaged at room temperature on upright microscopes with direct water immersion objectives. Wide-field epifluorescence data were collected via objectives with numerical apertures (NAs) ranging from 0.9 to 1.1 with cooled CCD cameras with 6.7- $\mu\text{m}$ -wide pixels. FRAP experiments and optical sectioning were performed with a Zeiss Pascal scanning confocal microscope equipped with a 0.95-NA objective.

Release was quantified as the loss in bouton neuropeptide fluorescence. This was possible because photobleaching was minimal in these studies. Furthermore, because we imaged axons and multiple *en passant* boutons in each experiment, our time-lapse imaging revealed that depletion of peptide content occurred without redistribution of peptidergic vesicles into axons, in accordance with previous experiments<sup>23</sup>. For ease of presentation, only representative single boutons are shown in the figures. Furthermore, some figures use pseudocolor scales generated by Image J or Zeiss Pascal confocal software. Units in these figures are arbitrary, but the vertical dimension is linear from minimal to maximal values in the figure.

We initially discovered the effect of activity on peptidergic vesicle motion in type Ib boutons by examining time-lapse movies. However, for analysis, it was necessary to develop an unbiased indicator of vesicle dynamics. Therefore, we made use of the pixel-by-pixel correlation coefficient (CC) between neighboring images, acquired at 3-s intervals, to quantify the degree of vesicle movement. Quantification of such fluctuations is utilized in fluorescence correlation spectroscopy (FCS), a method that is analogous to noise analysis for the study of channels. However, deducing diffusion coefficients by FCS requires rigorous geometrical boundary conditions that are not apparent for type Ib boutons. Therefore, we characterized LDCV motion by calculating a mobility index equal to  $1 - \text{CC}$ . As this is a statistical value, we acquired a series of images under one experimental condition and used the mean value of the mobility index determined from the series of images. A number of internal controls indicate that the mobility index accurately reflects vesicle motion, and not release. First, relative values agreed with qualitative estimates from inspection of time-lapse movies. Second, the stimulus induced change in the mobility index was unaffected by inhibiting release with NEM. Third, the time course for the change in the mobility index did not parallel the time course of release.

#### ACKNOWLEDGMENTS

This research was supported by US National Institutes of Health grant NS32385 (to E.S.L.) and Oklahoma Center for Science and Technology grant HR03-0485 (to R.S.H.). We thank C. Ziegler for technical assistance.

#### COMPETING INTERESTS STATEMENT

The authors declare that they have no competing financial interests.

Received 23 September; accepted 26 October 2004

Published online at <http://www.nature.com/natureneuroscience/>

- Zupanc, G.K. Peptidergic transmission: from morphological correlates to functional implications. *Micron*. **27**, 35–91 (1996).
- Hokfelt, T., Broberger, C., Xu, Z.Q., Sergeev, V., Ubink, R. & Diez, M. Neuropeptides—an overview. *Neuropharmacology* **39**, 1337–1356 (2000).
- Taghert, P.H. & Veenstra, J.A. *Drosophila* neuropeptide signaling. *Adv. Genet.* **49**, 1–65 (2003).

- Whim, M.D. & Lloyd, P.E. Frequency-dependent release of peptide cotransmitters from identified cholinergic motor neurons of *Aplysia*. *Proc. Natl. Acad. Sci. USA* **86**, 9034–9038 (1989).
- Martin, T.F. The molecular machinery for fast and slow neurosecretion. *Curr. Opin. Neurobiol.* **4**, 626–632 (1994).
- Holt, M., Cooke, A., Neef, A. & Lagnado, L. High mobility of vesicles supports continuous exocytosis at a ribbon synapse. *Curr. Biol.* **14**, 173–183 (2004).
- Rea, R. *et al.* Streamlined synaptic vesicle cycle in cone photoreceptor terminals. *Neuron* **41**, 755–766 (2004).
- Henkel, A.W., Simpson, L.L., Ridge, R.M. & Betz, W.J. Synaptic vesicle movements monitored by fluorescence recovery after photobleaching in nerve terminals stained with FM1-43. *J. Neurosci.* **16**, 3960–3967 (1996).
- Kraszewski, K., Daniell, L., Mundigl, O. & DeCamilli, P. Mobility of synaptic vesicles in nerve endings monitored by recovery from photobleaching of synaptic vesicle-associated fluorescence. *J. Neurosci.* **16**, 5905–5913 (1996).
- Ng, Y.K., Lu, X. & Levitan, E.S. Physical mobilization of secretory vesicles facilitates neuropeptide release by nerve growth factor-differentiated PC12 cells. *J. Physiol.* **542**, 395–402 (2002).
- Becherer, U., Moser, T., Stuhmer, W. & Oheim, M. Calcium regulates exocytosis at the level of single vesicles. *Nat. Neurosci.* **6**, 846–853 (2003).
- Zucker, R.S. & Regehr, W.G. Short-term synaptic plasticity. *Annu. Rev. Physiol.* **64**, 355–405 (2002).
- Seward, E.P., Chervenskaya, N.I. & Nowycky, M.C. Exocytosis in peptidergic nerve terminals exhibits two calcium-sensitive phases during pulsatile calcium entry. *J. Neurosci.* **15**, 3390–3399 (1995).
- Brezina, V., Church, P.J. & Weiss, K.R. Temporal pattern dependence of neuronal peptide transmitter release: models and experiments. *J. Neurosci.* **20**, 6760–6772 (2000).
- Ludwig, M. *et al.* Intracellular calcium stores regulate activity-dependent neuropeptide release from dendrites. *Nature* **418**, 85–89 (2002).
- Steyer, J.A., Horstmann, H. & Almers, W. Transport, docking and exocytosis of single secretory granules in live chromaffin cells. *Nature* **388**, 474–478 (1997).
- Olofsson, C.S. *et al.* Fast insulin secretion reflects exocytosis of docked granules in mouse pancreatic B-cells. *Pflugers Arch.* **444**, 43–51 (2002).
- Duncan, R.R. *et al.* Functional and spatial segregation of secretory vesicle pools according to vesicle age. *Nature* **422**, 176–180 (2003).
- Han, W., Ng, Y.K., Axelrod, D. & Levitan, E.S. Neuropeptide release by efficient recruitment of diffusing cytoplasmic secretory vesicles. *Proc. Natl. Acad. Sci. USA* **96**, 14577–14582 (1999).
- Ng, Y.K. *et al.* Unexpected mobility variation among individual secretory vesicles produces an apparent refractory neuropeptide pool. *Biophys. J.* **84**, 4127–4134 (2003).
- Burke, N.V. *et al.* Neuronal peptide release is limited by secretory granule mobility. *Neuron* **19**, 1095–1102 (1997).
- Levitan, E.S. Using GFP to image peptide hormone and neuropeptide release in vitro and in vivo. *Methods* **33**, 281–286 (2004).
- Rao, S., Lang, C., Levitan, E.S. & Deitcher, D.L. Visualization of neuropeptide expression, transport, and exocytosis in *Drosophila melanogaster*. *J. Neurobiol.* **49**, 159–172 (2001).
- Atwood, H.L., Govind, C.K. & Wu, C.F. Differential ultrastructure of synaptic terminals on ventral longitudinal abdominal muscles in *Drosophila* larvae. *J. Neurobiol.* **24**, 1008–1024 (1993).
- Jia, X.X., Gorczyca, M. & Budnik, V. Ultrastructure of neuromuscular junctions in *Drosophila*: comparison of wild type and mutants with increased excitability. *J. Neurobiol.* **24**, 1025–1044 (1993).
- Husain, Q.M. & Ewer, J. Use of targetable GFP-tagged neuropeptide for visualizing neuropeptide release following execution of a behavior. *J. Neurobiol.* **59**, 181–191 (2004).
- Heifetz, Y. & Wolfner, M.F. Mating, seminal fluid components, and sperm cause changes in vesicle release in the *Drosophila* female reproductive tract. *Proc. Natl. Acad. Sci. USA* **101**, 6261–6266 (2004).
- Jan, L.Y. & Jan, Y.N. Properties of the larval neuromuscular junction in *Drosophila melanogaster*. *J. Physiol.* **262**, 189–214 (1976).
- Stewart, B.A., Atwood, H.L., Renger, J.J., Wang, J. & Wu, C.F. Improved stability of *Drosophila* larval neuromuscular preparations in haemolymph-like physiological solutions. *J. Comp. Physiol. A* **175**, 179–191 (1994).
- Barclay, J.W., Atwood, H.L. & Robertson, R.M. Impairment of central pattern generation in *Drosophila* cysteine string protein mutants. *J. Comp. Physiol. A* **188**, 71–78 (2002).
- Cattaert, D. & Birman, S. Blockade of the central generator of locomotor rhythm by noncompetitive NMDA receptor antagonists in *Drosophila* larvae. *J. Neurobiol.* **48**, 58–73 (2001).
- Pfister, K.K., Wagner, M.C., Bloom, G.S. & Brady, S.T. Modification of the microtubule-binding and ATPase activities of kinesin by *N*-ethylmaleimide (NEM) suggests a role for sulfhydryls in fast axonal transport. *Biochemistry* **28**, 9006–9012 (1989).
- Phelps, K.K. & Walker, R.A. *N*-ethylmaleimide inhibits Ncd motor function by modification of a cysteine in the stalk domain. *Biochemistry* **38**, 10750–10757 (1999).
- Perry, S.V. & Cotterill, J. The action of thiol reagents on the adenosine-triphosphatase activities of heavy meromyosin and L-myosin. *Biochem. J.* **96**, 224–230 (1965).
- Delgado, R., Maureira, C., Oliva, C., Kidokoro, Y. & Labarca, P. Size of vesicle pools, rates of mobilization, and recycling at neuromuscular synapses of a *Drosophila* mutant, *shibire*. *Neuron* **28**, 941–953 (2000).
- Rizzoli, S.O. & Betz, W.J. The structural organization of the readily releasable pool of synaptic vesicles. *Science* **303**, 2037–2039 (2004).
- Bantignies, F., Goodman, R.H. & Smolik, S.M. Functional interaction between the coactivator *Drosophila* CREB-binding protein and ASH1, a member of the trithorax group of chromatin modifiers. *Mol. Cell Biol.* **20**, 9317–9330 (2000).

